Microcalcification Detection in Mammograms Using Difference of Gaussians Filters and a Hybrid Feedforward-Kohonen Neural Network

Juan F. Ramirez-Villegas, Eric Lam-Espinosa, and David F. Ramirez-Moreno
Departament of Automatics and Electronics
Universidad Autonoma de Occidente
Cali, Colombia
e-mails: juanfelipe.rv@gmail.com; elam044@hotmail.com; dramirez@uao.edu.co

***Abstract*–This work develops a microcalcifications' detection system in mammograms by using difference of Gaussians filters (DoG) and artificial neural networks (ANN). The digital image processing proposed show the basic wavelet-based behavior of DoG as a mother function frequently used in several vision tasks, and in this case, used in order to enhance the microcalcifications' traces in standard mammograms and further to achieve its detection via ANN. In order to achieve this, a segmentation algorithm is implemented for reaching a threshold in already processed images, and finally, the resultant information is given to the ANN. The neural network used to perform the detection is a hybrid feedforward-Kohonen one, implemented with a hard-limit transfer function in the first layer and a self-organizing map (SOM) responsible for microcalcifications' topologic adjustment in the second layer. Basically, this clustering method gave us a robust solution of the problem and the detection was performed efficiently. There are no considerations relative to morphologic analysis of microcalcifications for diagnosis in this work.**

Keywords– Microcalcification, mammogram, Difference of Gaussians filters, artificial neural networks, hard limit function, self-organizing map.

I. INTRODUCTION

Intelligent systems are powerful processing techniques, that have been helpful in improving medical diagnosis in relation to various pathologies associated with atypical signs in different organs.

According to the article *"Casos Nuevos de Cancer en el Instituto Nacional de Cancerologia, Colombia, 2002"* [1], 2002, there were 4990 new cancer cases, 13% more than the last year and 12.2% corresponding to breast cancer. Furthermore, between 30 and 50 years-old breast tumors are predominant according to a cancer decease report in Colombia, 2001 [2]. The early and accurate diagnosis of this pathology is critical in order to decrease the mentioned rates.

The definition of image processing is the manipulation of a numerical representation of the image by a computer, applying a series of operations in order to obtain a desired result [3]. Processing methods such as high pass filtering in different modalities are implemented in standard radiology, mammography, tomography, and magnetic resonance for image characteristics enhancing.

As it is a very difficult job, there is some background related to how radiologists achieve the identification of pathological signs in mammograms: Usually, the information given by a mammogram is not obvious for the radiologists; thereby manual reading of a mammogram turns into a time demanding and high-concentration task. Usually, the performance of the radiologists varies from 65-85% effectiveness [4]-[5]. In many cases there are two types of errors: False positives (FP), which consists of the detection of a sign that appears to be malign, this usually lead to unnecessary interventions; and false negatives (FN), which are detections of malign signs that are classified as benign by radiologists. There are some methods to avoid this problem such as a decision based on the examination of the mammogram by two different radiologists; nevertheless, the performance does not show clear improvements [6].

A mammographic image is characterized by a high spatial resolution which is adequate enough to detect subtle fine-scale signs such as microcalcifications (μCas). On the other hand, the analysis of mammographic images is a complex and cumbersome task which requires highly specialized radiologists [7]. In radiological practice, nearly all images are not able to provide the information required by specialists, which produces inaccurate interpretations in no few cases, due to visual fatigue and other factors. Although image acquisition techniques for medical applications have been improved, as a matter of fact, computer aided diagnosis (CAD) systems implementation is necessary to achieve these tasks. CAD can be applied to digital images obtained from a set of imaging modalities, to address a variety of diagnostic problems. CAD systems have been implemented to support the detection and characterization of breast lesions from digital mammography [8]. A simple block diagram to describe the functioning of CAD systems is presented in Fig. 1.

Most of computer aided diagnosis (CAD) systems implement different intelligent algorithms to perform the detection of alterations or signs hardly perceptible in images. The artificial neural networks (ANN) as neurobiological inspired models have several applications in

mammary pathologies detection. Some methods used regularly such as Radial basis functions (RBF) or Kohonen's SOM [9] give robust solutions in several diagnosis tasks, in addition to powerful classifiers such as Multi-Layer Perceptron (MLP-BP) networks [7].

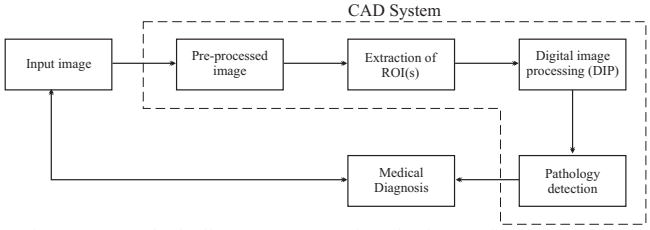

Figure 1. Block diagram representing the interaction between CAD and the specialist in pathology diagnosis.

These models follow principles found in neurocomputation. Cortical neural representations appear spatially organized, characteristic that SOFM (Self-Organizing Feature Maps) networks models [8] try to reproduce [9]. In consequence, given the network structure and a good dynamics, the input space feature content is enough to force maps formation [11].

On the other hand, neurophysiological experiments provide some evidence about the visual pathway in relation to spatial and high frequency discrimination endowed with highly non-linear operations in layers of neurons (e.g., retinal ganglion cells) that can be approximately implemented by a set of masks around the visual field which allows to detect edges, orientations and moreover, contrast details between and on different surfaces [12]. These neurobiological bases are related in the literature to the LoG (Laplacian of Gaussian) filters implementation, and to Gaussian kernels in DoG implementations. Spatial and frequency domain filtering techniques for detecting signs in images are referred to extensively in the literature and textbooks [13], [17].

This work proposes a computational tool for microcalcifications' detection in mammograms using difference of Gaussian (DoG) filtering and artificial neural networks (ANN), as a system with potential applications to computer aided diagnosis. The ANN proposed is a hybrid multilayer network with unsupervised learning in the last layer using Kohonen's self organizing maps (SOM) algorithm [9].

II. Methods and Materials

A. Contrast Enhancement

In order to generate a contrast-enhanced input image, an Adaptative Histogram Equalization (AHE) is performed. This method exhibits improvements over the Local-Area Histogram Equalization (LAHE), which presents noise magnification due to standard histogram equalization computed for each pixel taking into account its neighborhood (contextual region).

In order to decrement the computational load, equalization can be computed only for some pixels (and its context regions), as the image is divided into a mosaic; thereby, the modified pixel is the central pixel, and the others are obtained using a standard bilinear interpolation method. In this way, each contextual region will affect with its equalization another spatial zone of double its length.

The final value of each pixel will be obtained applying the pixel mapping according to (1).

$$L(i) = C\left[E\,N_{--}(i) + (1-E)N_{+-}(i)\right] + (1-C)\left[E\,N_{-+}(i) + (1-E)N_{++}(i)\right], \quad (1)$$

Where N_{--} is the mapping of the left superior area, N_{-+} is the mapping of the left inferior area, and so on. An example of AHE applied to contrast-enhancement of a mammogram is illustrated by Fig. 2.

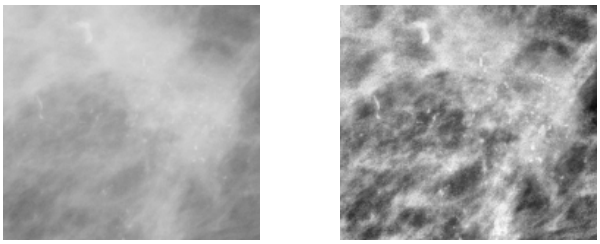

Figure 2. ROI of mammographic image (left). Contrast-enhanced image (right)

Fig. 2 shows clearly the effect of the contrast enhancement strategy. We can notice that original ROI has low contrast; the adaptive equalization produces an output image having grey values distributed throughout the intensity range. This technique can be applied to enhance the high frequency components of the image, i.e., microcalcifications due to the computations taken into account for central and contextual region pixels. In order to avoid the noise amplification a contrast limited-equalization can be performed, especially in homogeneous areas.

B. Background Suppression

In order to extract relevant characteristics of mammography images, it is not necessary to take the whole image, because usually microcalcifications are in some specific regions of interest (ROIs) which are represented as suspicious regions with high grey levels. In many applications ROI can be selected by a specialist if it is required for the image processing step.

The enhancement stage must be sensitive enough to emphasize small low-contrast objects while, at the same time, it must have the required specificity to suppress the background [7]. Usually the background corresponds to some smoothed fractions of the image provided by the tissue characteristics and image acquisition process; in consequence, these areas are softened regions of image which give no-relevant information about pathologies in many cases. Background suppression can be implemented by using high pass filtering.

In this work, the suppression is performed using difference of Gaussians filters according to (2), where $\boldsymbol{I}$ is the ROI, and the additional term of convolution is the filter function. In this way, the convolution corresponds to a smoothed version of the same ROI.

$$I_r(x) = I(x) - DoG(x) \otimes I(x). \quad (2)$$

DoG (Difference of Gaussians) is a linear filter implemented in several artificial vision tasks, which works by subtracting two Gaussian blurs of the image corresponding to different functions widths (Fig. 3). The filter equation is represented by (3) where $\boldsymbol{x}$ is the vector of positions in the image, so that $x = (x, y)$.

$$DoG(x) = A_1 \frac{1}{2\pi\sigma_1^2} \exp\left[-\frac{x^2}{2\sigma_1^2}\right] - A_2 \frac{1}{2\pi\sigma_2^2} \exp\left[-\frac{x^2}{2\sigma_2^2}\right]. \quad (3)$$

The enhancing process with the DoG works in both the spatial and frequency domain. Fig. 3 shows the filter behavior in the spatial and frequency domain with different standard deviations and A_n peaks set to unity. Indeed, the performance of the filter is conditioned by parameters σ_n and in one case, A_n peaks estimation. In (3), standard deviation σ_n is related with lateral inhibition of the filter, while the term which follows A_n peaks normalizes the sum of mask elements to unity in the image processing. For this research, some mathematical expressions used to determine the DoG parameters according to microcalcifications' average width and Marr's ratio [15] for different kernels were used. These expressions are available in the literature and they make the background suppression performance high [14].

For a target of size (average width) t, (4)-(5) can be used.

$$\sigma_2 = \frac{t}{2}, \quad (4)$$

and from Marr's ratio:

$$\sigma_1 = \frac{t}{1.6}. \quad (5)$$

As seen in Fig. 3, the algorithm to obtain the filtered regions represented by (2) is selective enough to give some particularities such as microcalcifications because of the background suppression of the ROIs of the input image in the spatial domain. On frequency domain, the basic effect of the filter is almost the same, the microcalcifications' frequency components are enhanced based on a band pass-like filter which discards all but a handful of spatial frequencies that are present in the original image.

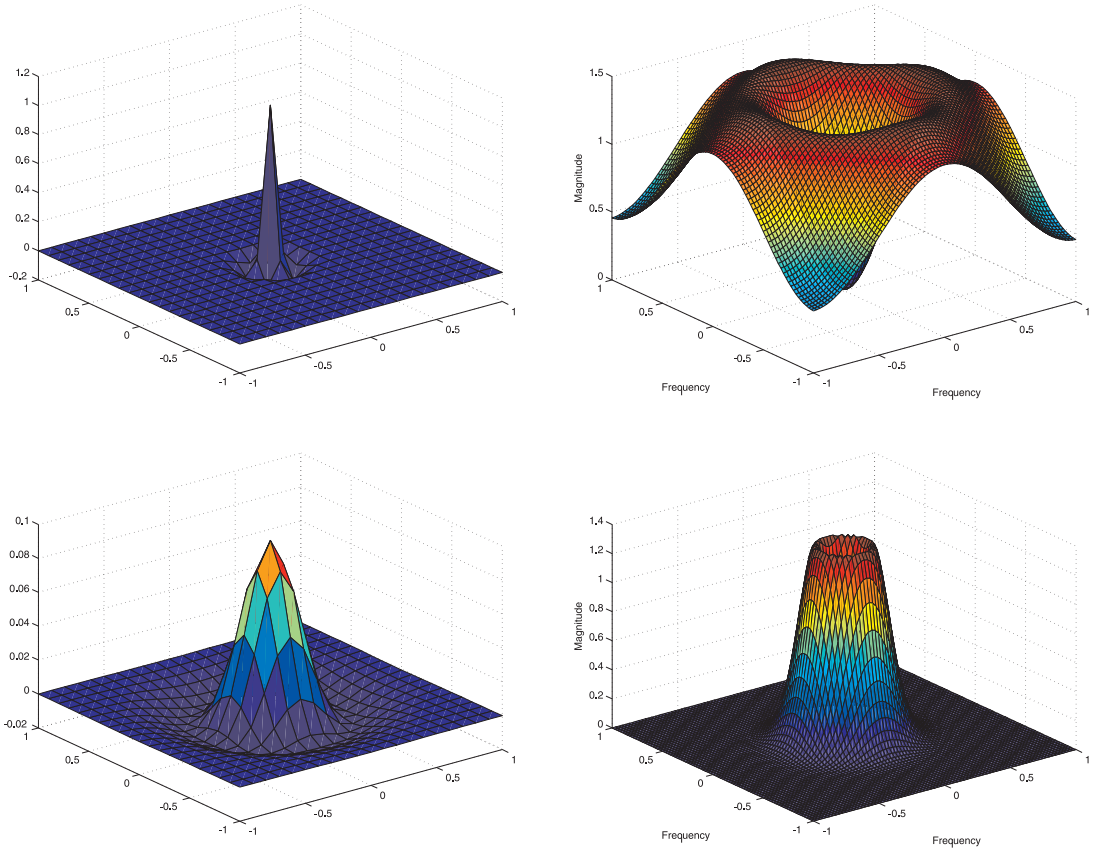

(a) (b)

Figure 3. (a) DoG kernels with $\sigma_1 = \{0.3, 1.0\}$ and $\sigma_2 = \{0.48, 1.6\}$, respectively. (b) Frequency response of DoG kernels.

In other words, the subtraction of the two blurred versions (two Gaussians) of the images leads to obtain high frequency spatial information suppressed, but it preserves spatial information which is contained into a specific range of frequencies, microcalcifications are in this range of frequencies.

There are some approaches that have applied DoG filters for microcalcification detection, as it is useful for avoiding some FPs [14], [18]; basically the ROIs are highlighted and the performance becomes better when another complementary algorithm.

Since the first approximation to enhance microcalcification detection explained in this work is in some cases useful to specialists, residual noise reduction is the following step. There are several noise reduction techniques available in the literature [12]-[14], [19]. In some research, noise modelling is available by using statistical parametrization [16] and some others use MLP-BP neural networks as classifiers [7].

C. Image Segmentation Problem

Usually, an important problem is emphasizing image regions, which summarizes into threshold estimation based on statistical information given by ROI(s) or already processed images. Frequently the processing in the collected images by using DoG filters is varying in quality (satisfactory quality and poor quality); thereby, this establishes some individuality of the grey level contrast [17] provided by the tissue characteristics and image acquisition process. In consequence, regions of images such as mammograms [20] are suitable with several segmentation algorithms. The pattern classifier via ANN using image segmentation must be specific enough to avoid false positives in the enhancing process. The whole enhancing procedure proposed in this work is illustrated by Fig. 4.

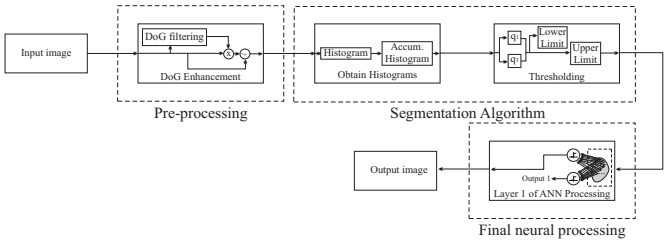

Figure 4. Block diagram of the whole enhancing procedure. We assume that input image is a contrast-enhanced one by applying adaptative histogram equalization.

The distinction between emphasized regions of mammogram is done by the first layer of the ANN. In order to achieve this, a segmentation algorithm based on the histogram of the processed image is implemented; the algorithm seeks to raise a threshold into the image grey levels (as seen in Fig. 4). The segmentation algorithm proposed in this work is summarized by the following steps [9]:

Step 1. Calculate the histogram of the processed ROI for each grey level r_k with (6).

$$p(r_k) = \frac{n_k}{n}, \tag{6}$$

Step 2. Accumulate the histogram for each grey value as follows:

$$p_A(i) = \sum_{k=0}^{i-1} p(k), \tag{7}$$

Step 3. Calculate the grey level corresponding to the first quartile (q_1) position on the sample of N pixels as shows (8).

$$Pq_1 = 0.25N, \tag{8}$$

Step 4. Calculate the grey level corresponding to the third quartile (q_3) position on the sample of N pixels with (9).

$$Pq_3 = 0.75N, \tag{9}$$

Step 5. Calculate the lower limit L_1 with (10).

$$L_1 = q_1 - 1.5(q_3 - q_1), \tag{10}$$

Step 6. Calculate the upper limit U_1 with (11).

$$U_1 = q_1 + 1.5(q_3 - q_1), \tag{11}$$

After threshold h is reached, the following step is to adjust the zero between the two different pixel classes by subtracting the calculated threshold from each pixel of the resultant image.

D. Microcalcification Detection Performance

The neural network proposed for microcalcification detection in this work is a hybrid feedforward-Kohonen network (see Fig. 5), composed by two hard-limit transfer function nodes on the first layer as shows (12), which discriminates between suspect zones of the mammogram by applying the procedure already explained (Fig. 4). In this way, the first node of the first layer will be excited for atypical grey values (microcalcifications) and the second one for grey values between the typical ranges (noise). In one case postsynaptic potential in the first neuron will be a positive integer while in the second one, will be zero and vice versa; finally, the typical grey values are disqualified and the other information of the resultant image is transferred to the second layer in order to generate the topological adjustment of microcalcifications.

$$hard\lim(x) = \begin{cases} 1, & x \geq 0 \\ 0, & otherwise \end{cases}, \tag{12}$$

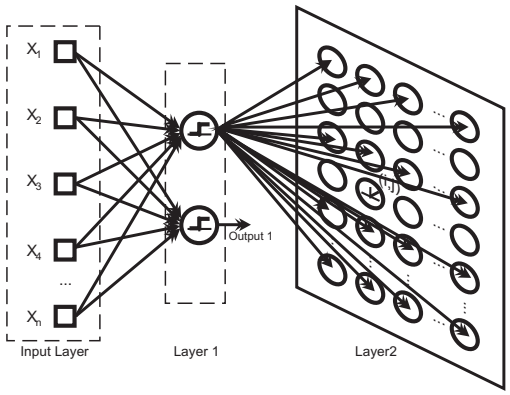

Figure 5. Hybrid feedforward-Kohonen ANN.

The second layer of the ANN is an unsupervised learning layer which is responsible for the microcalcifications topologic adjustment using the Kohonen network algorithm; chosen as a known clusterer and categorizer. In this model, neurons are organized into an unidirectional architecture, where first layer consists of *m* neurons (if we consider each pixel of the image) that operate as buffers distributing the information from input space to neurons on last layer which generates the feature map; these neurons work in parallel [10].

On the other hand, this work takes into account the following criteria for second layer computation:

- *Winner Neurons.* The Euclidean distance defined between the synaptic weights (w_{ij}) of the neurons and the input patterns (x_j), according to (13). In this way, a winner neuron is chosen as the neuron with the minimum Euclidean distance to one target; then, in different iterations, the synaptic weights for each neuron are updated according to (14). The weight updating depends on learning rate function $\alpha(t)$ and neighborhood function $h(.)$.

$$E = \min\left\|w_{ij} - x_{ij}\right\| = \min\left(\sqrt{(w_i - x_i)^2 + (w_j - x_j)^2}\right), \quad (13)$$

$$w_{ijk}(t+1) = w_{ijk}(t) + \alpha(t)h(|i-g|,t)\left(x_k(t) - w_{ijk}(t)\right), \quad (14)$$

- *Learning Rate.* A learning rate (α) is a decreasing function and describes how much neurons rotate or approximate to input patterns according to (15). Indeed, the synaptic weights on the input space find regularities in the input space feature content and organize it into clusters or groups of patterns with similar characteristics. In this way, at the beginning of the learning the synaptic weights are randomly distributed; once the learning process has began, the neurons move to the targets until the desired performance is reached. Usually, in order to generate the final desired stable state of the network, initial (α_0) and final (α_f) learning rates must be small values ($\alpha_f < \alpha_0$); the learning parameters estimation is not a cumbersome task and can be determined according to parameters commonly referred in literature [8], [10].

$$\alpha(t) = \alpha_0 + (\alpha_f - \alpha_i)\frac{t}{N}, \quad (15)$$

- *Neighborhood Factor.* Finally a proximity factor (β) or neighborhood radius, expresses what are the allowed neighborhood to be associated with the winner neuron in each iteration, as shown in (16). Although there are several mathematical functions to describe the neighbourhood denoted as $h(.)$ in (14) when Kohonen's algorithm is applied, DoG functions, Gaussians and rectangular functions are mainly implemented as a general statement as they describe with accurate response the adaptation strength of the winner neuron to each other. The neighborhood function taken into account for this work is a unit step function, because is the most simple and gives a robust solution of the problem.

Depending on the number of neurons in the input space, initial (β_0) and final (β_f) proximity factors usually change; they can be estimated according to the neurons' distribution or in a heuristic way.

$$\beta(t) = \beta_0\left(\frac{\beta_f}{\beta_0}\right)^{\frac{t}{N}}, \quad (16)$$

In these (15) and (16), t represents the actual iteration and N the total number of train cycles. The initial and final learning parameters appear referred in literature [10].

III. Results

The mammographic images were taken from The Mini-MIAS Database of Mammograms [21], that provides appropriate details of the pathologies and general characteristics of the mammograms: The MIAS database reference number, character of background tissue (as it can be fatty, fatty-glandular and dense-glandular), class of abnormality present (as it can be calcification, well-defined/circumscribed masses, spiculated masses, ill-defined masses, architectural distortion, asymmetry or normal), severity of abnormality (as it can be benign or malignant).

For the artificial neural network simulation and imaging processing, we used MatLab™ v. 7.4.0. The general results are divided in two parts, corresponding to two examples to show the processing for different mammographic images obtained form the database.

The images in Fig. 6 and Fig. 8 correspond to the original image, to ROI extraction and to the initial processing made with difference of Gaussians (DoG) filters. The region of the image in study contains the microcalcifications and the filtering performance is relatively good in one case, although its specificity is not the best to achieve the task.

Finally with the previous information Fig. 7 and Fig. 9 are obtained, which contains the images after the neural processing. The specificity of the *DoG* filter increments with the discrimination of patterns by the first layer of the artificial neural network (segmentation), making the results more accurate according to microcalfications enhancement.

Additionally, it is important to consider that the topological adjustment made in the Kohonen layer of the

network is accurate and suitable for the application (Fig. 7 and Fig. 9, C). The number of neurons in the input space was limited (Fig. 9, B) according to the number of possible pathological signs in the input space.

A. Example 1

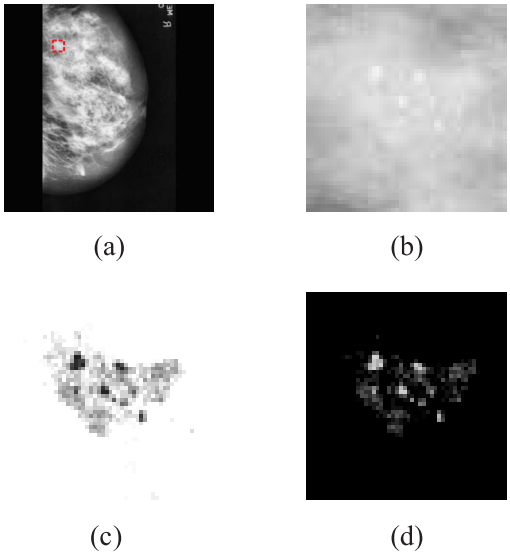

Figure 6. (a) Input image (mdb236 in the database); (b) Region of interest of the image, the red section in (a); (c) Smoothed version of image using DoG filters; (d) Resultant image processing according to (1).

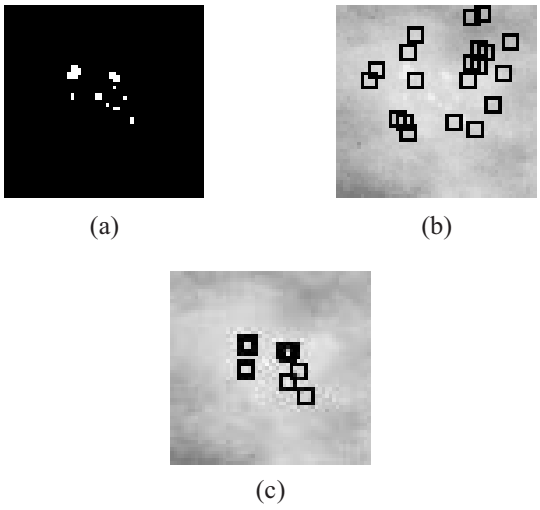

Figure 7. (a) Grey level discrimination by the first layer of the ANN; (b) Initial neurons' synaptic weights (black squares, Kohonen layer) randomly distributed on input space; (c) Topologic adjustment of Microcalcifications by Kohonen layer.

B. Example 2

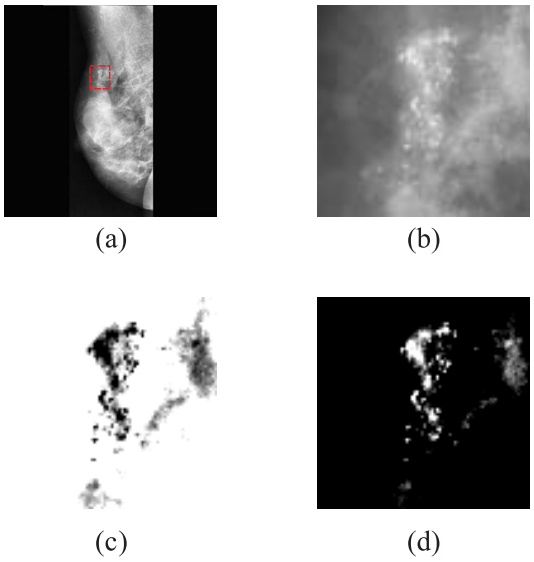

Figure 8. (a) Input image (mdb241 in the database); (b) ROI of the image, the red section in (a); (c) Smoothed version of image (DoG processing); (d) Resultant image (Image subtraction from smoothed version).

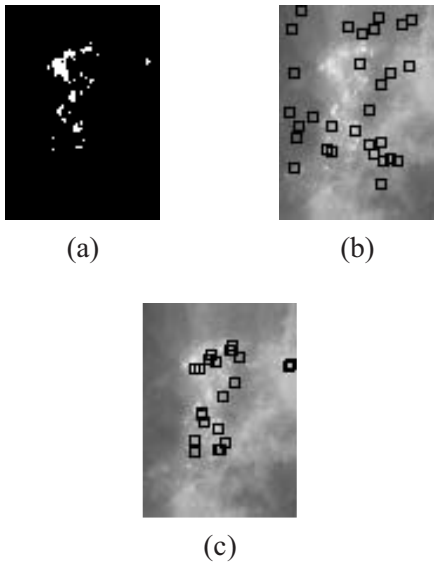

Figure 9. (a) Grey level discrimination by the first layer of the ANN; (b) Initial neurons' synaptic weights (black squares, Kohonen layer) randomly distributed on input space; (c) Topologic adjustment of Microcalcifications by Kohonen layer (detection performance).

The performance of the proposed system is shown by FROC curves in Fig. 10 and Fig. 11. FROC curves are mainly implemented to objectively evaluate and analyse image processing algorithms, such as imaging CAD algorithms. Increasing the sensitivity of the algorithm can lead to false positives when reaching the detection of subtle signs. The experimental results of this algorithm were directed to how the proposed algorithm can improve the

diagnosis of pathological signs. All the performance results as well as the image processing and detection ones were made using the test sets (selected from the Mini-MIAS database).

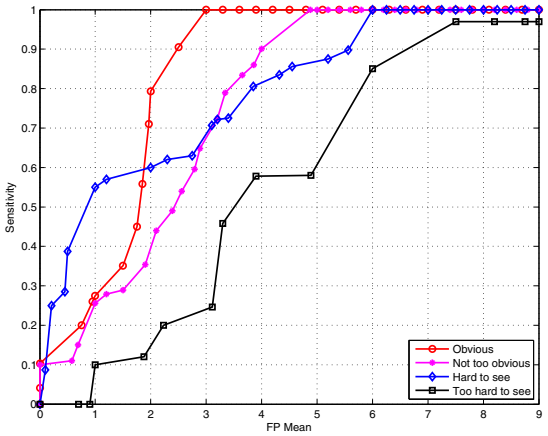

Figure 10. Curves showing the proposed method performance using the Mini-MIAS database according to the microcalcifications subtleness degree.

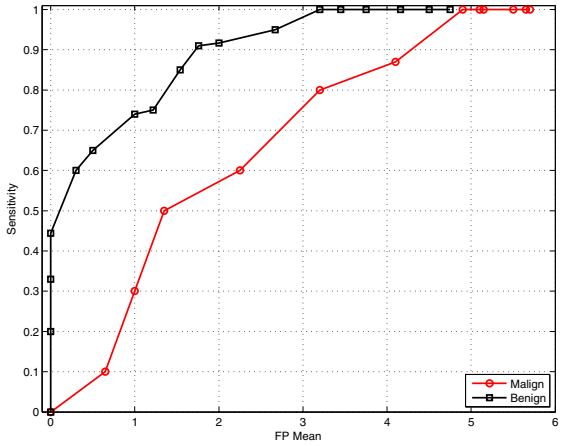

Figure 11. Curves showing the proposed method performance using the Mini-MIAS database according to the benignancy/malignancy of the pathology.

It is interesting to see that malignant microcalcifications are harder to detect than benign because they appear to be more subtle, which is attributable to the contrast conditions of pathological/non-pathological areas on the mammograms, as they describe the tissue characteristics. On the other hand, ROIs extraction introduces different variations on the detection performance, as it includes/excludes some possible FPs detection. Even when the signs are too hard to detect, the FROC curves are relatively close and FPs mean is not above of 9 with a performance of 97.5% in the hardest cases.

The malignancy of the pathologies in diagnostic images in different modalities (MR, retinograms, mammograms, chest radiographies) should be one of the main topics in CAD evaluations, as it provides information about how specific are the techniques or approaches in detection of pathologies; thereby they can be characterized by powerful descriptors such as the size of the signs, character of the background tissue, characterization of the abnormality (e. g. single or clustered microcalcifications), approximated radius of the pathology in each image. The performance of the neural network was achieved using 500 train cycles for the two-dimensional Kohonen layer, in which location of the possibly pathological regions are given.

IV. Discussion and Conclusions

In general, the computational model shown in this work presents satisfactory results in microcalcifications detection; the filtering applied has shown accurate responses from a mammogram to another (Fig. 6 and Fig. 8). The dynamics of the network as a category generator on input space is non-linear and also neurobiologically inspired; the artificial neural network proposed in this paper presents a higher robustness and tolerance to failures.

MLP/SVM approximations can be generated by extracting some pathological/non-pathological ROIs and extracting a group of characteristics by parametrization of those ROIs or standard group of matrixes from some mammograms. The network can be trained using background spots, defects of the filming/digitalization process and so on. The expected sensitivity in the process is about 85-94% (R. M. Rangayyan et. al., 2007) due to the generalization degree exposed by a MLP/SVM in classification tasks.

There are other methods used in several clustering tasks. Growing Neural Gas (GNG) is a Kohonen algorithm method-based, which is an unsupervised incremental clustering algorithm. This algorithm is used for finding topological structures that closely reflects the structure of the input features distribution [24]. The last algorithm explained makes detection system accuracy higher, but the computational load too. The results obtained in this work are a starting platform for mammary pathology detection systems and other computer aided diagnosis methods implementation using digital image processing and artificial intelligence in Colombia.

The performance of the method proposed in this approach can be compared with other methods available in the literature [5]-[7], [16]; these methods shows clear improvements on the pathological signs detection, nevertheless, the proposed algorithm appear to be versatile and efficient in terms of computational load as well as reaching the objective.

On the other hand, this paper has shown that advanced techniques of image processing and microcalcification detection are useful in computer aided diagnosis. The intelligent systems development combined with health specialists' knowledge improve diagnostics associated to different pathologies. In this work, a neural network due to a segmentation algorithm has allowed enhancing characteristics of the images to be better than just using DoG filtering; this procedure is also suitable with detection of clustered microcalcifications due to its robustness. Additionally, providing diagnosis in early stages of development of the pathology, this work is a step to achieve a low prevalence in deceases caused by breast cancer.

Previous work has shown that DoG is a really powerful processing technique [7], [14], nevertheless, it leads to obtain relatively high FP rates when no refining algorithm is applied, such as classification via neural networks; segmentation algorithms can be applied in order to increase the general sensitivity too, the approach shown in this work, consists on combining DoG performance, segmentation and neural networks to increase the sensitivity and adaptability of the imaging system.

Morphological description of microcalcifications considers terms such as: Typically benign, undetermined and probably malign [6]. This new component will give accurately results in helping medical diagnosis. These topics should be useful in further researches.

ACKNOWLEDGEMENT

We acknowledge the support of:

Dr. Odelia Schwartz from the Department of Neuroscience, Albert Einstein College of Medicine in New York City, USA.

Kristy A. Godoy-Jaimes, B. Eng., from Universidad Autonoma de Occidente, Cali, Colombia

REFERENCES

[1] F. L. Ochoa, L. P. Montoya, "Mortalidad por cáncer en Colombia 2001", Available online: http://www.ces.edu.co/Descargas%5CPubl_Med_Vol18_2%5CCancer.pdf

[2] C. Pardo, R. Murillo, M. Piñeros, M. A. Castro, "Casos nuevos de cáncer en el instituto nacional de cancerología", Colombia, 2002, Available online:http://www.incancerologia.gov.co/documentos/10_10_2007_7_24_34_AM_rcc2003v07n3a02_Resumen.pdf.

[3] P. Arena, A. Basile, M Bucolo, L. Fortuna, "Image processing for medical diagnosis using CNN", Nuclear Instruments and Methods in Physics Research A 497, pp. 174–178, 2003.

[4] H.D. Cheng, X.J. Shi, R. Min, L.M. Hu, X.P. Cai, H.N. Du, "Approaches for automated detection and classification of masses in mammograms", Pattern Recognition 39, pp. 646 – 668, 2006.

[5] R. M. Rangayyana, F. J. Ayresa, J. E. Leo Desautels, "A review of computer-aided diagnosis of breast cancer: Toward the detection of subtle signs", Journal of the Franklin Institute 344, pp. 312–348, 2007.

[6] A. Vilarrasa-Andrés, Sistema inteligente para la detección y diagnóstico de patología mamaria, PhD Thesis, Dept. de radiología y medicina física, Universidad Complutense de Madrid, Madrid, España, 2006.

[7] L. Bocchi, G. Coppini, J. Nori, G. Valli, "Detection of single and clustered microcalcifications in mammograms using fractals models and neural networks", Medical Engineering & Physics 26, pp. 303–312, 2004.

[8] J. Stoitsis, I. Valavanis, S. G. Mougiakakou, S. Golemati, A. Nikita, K. S. Nikita, "Computer aided diagnosis based on medical image processing and artificial intelligence methods", Nuclear Instruments and Methods in Physics Research A 569, pp. 591–595, 2006.

[9] T. Kohonen, Self Organized Formation of Topologically Correct Feature Maps, Biological Cybernetics 43, pp. 59-69, 1982.

[10] J. Hertz, Introduction to the Theory of Neural Computation, Westview Press, 1991.

[11] S. Haykin, Neural Networks: A Comprehensive Foundation, Second Edition, Prentice Hall, inc., 1999.

[12] J. C. Russ, The image processing handbook, CRC Press, 1992.

[13] R. C. Gonzalez, R. E. Woods, S. L. Eddins, Digital image processing using MATLAB, First Edition, Prentice Hall, 2004.

[14] E. M. Ochoa, Clustered microcalcification detection using optimized difference of Gaussians (DoG), M.Sc. thesis, Dept. of the Air Force, Air Force Institute of Technology, Air University, Ohio, 1996.

[15] D. Marr, Vision: A computational investigation into the human representation and processing of visual information, W. H. Freeman and Co., San Francisco, 1982.

[16] F. W. Wheeler, A. G. Amitha-Perera, B. E. Claus, S. L. Muller, G. Peters, J. P. Kaufhold, "Micro-calcification detection in digital tomosynthesis mammography", SPIE Symposium on Medical Imaging, Conference on Image Processing, San Diego, February, 2006.

[17] A. W. Naji, A. R. Ramly, R. Ali, S. A. Rahman, M. L. Ali, "A segmentation algorithm based-on histogram equalizer for fingerprint classification system", Second International Conference on Electrical and Computer Engineering, ICECE, Dhaka, Bangladesh, 2002.

[18] W.E. Polakowski, D.A. Cournoyer, S.K. Rogers, M.P. DeSimio, D.W. Ruck, J.W. Hoffmeister, R.A. Raines, "Computer-aided breast cancer detection and diagnosis of masses using difference of Gaussians and derivative-based feature saliency", IEEE Trans. Med. Imaging 16 (6), pp. 811–819, 1997.

[19] M. Sonka, Image Processing, analysis and machine vision, University Press, 1993

[20] K. Rapantzikos and M. Zervakis, "Nonlinear enhancing and segmentation algorithm for the detection of age-related macular degeneration (AMD) in human eye's retina", Department of Electronics and Computer Engineering, Technical University of Crete, IEEE, pp. 1055-1058, 2001.

[21] J. Suckling, "The Mammographic Image Analysis Society Digital Mammogram Database", Exerpta Medica. International Congress Series 1069, pp. 375-378, 1994.

[22] M. Heath, K. Bowyer, D. Kopans, R. Moore, W. P. Kegelmeyer, The Digital Database for Screening Mammography, Proceedings of the Fifth International Workshop on Digital Mammography, M.J. Yaffe, ed., Medical Physics Publishing, pp. 212-218, 2001.

[23] M. Heath, K. Bowyer, D. Kopans, W. P. Kegelmeyer, R. Moore, K. Chang, S. M. Kumaran, Current status of the Digital Database for Screening Mammography, Digital Mammography, Kluwer Academic Publishers, Proceedings of the Fourth International Workshop on Digital Mammography, pp. 457-460, 1998.

[24] J. Holmström, Growing Neural Gas: Experiments with GNG, GNG with utility and supervised GNG, Uppsala M.Sc. thesis, Dept. of Information Technology, Uppsala University, Uppsala, 2002.